Soft Lubrication

J. M. Skotheim and L. Mahadevan

*Department of Applied Mathematics and Theoretical Physics, Centre for Mathematical Sciences, University of Cambridge,
Cambridge CB3 0WA, United Kingdom*
(Received 23 January 2004; published 18 June 2004)

We consider some basic principles of fluid-induced lubrication at soft interfaces. In particular, we quantify how a soft substrate changes the geometry of and the forces between surfaces sliding past each other. By considering the model problem of a symmetric nonconforming contact moving tangentially to a thin elastic layer, we determine the normal force in the small and large deflection limit, and show that there is an optimal combination of material and geometric properties which maximizes the normal force. Our results can be generalized to a variety of other geometries which show the same qualitative behavior. Thus, they are relevant in the elastohydrodynamic lubrication of soft elastic and poroelastic gels and shells, and in the context of biolubrication in cartilaginous joints.

Lubrication between two contacting surfaces serves to prevent adhesion and wear, and to reduce friction [1]. The presence of an intercalating "lubricating" fluid aids both, but gives rise to large hydrodynamic pressures in the narrow gap separating the surfaces and can thus lead to deformations of the surfaces themselves. For stiff materials such as metals, the pressure required for noticeable deformations is very large (~ 1 GPa) and under these conditions the lubricating fluid will exhibit non-Newtonian properties [2]. However, if these surfaces are soft, as in the case of gels and thin shells, elastohydrodynamic effects can become important when the fluid is still Newtonian since the pressure required to displace the surface is appreciably less. This type of situation is also common in mammalian joints where the synovial fluid serves as the lubricant between the soft thin cartilaginous layers which coat the much stiffer bones. Motivated by these observations, in this Letter we consider the coupling between fluid flow and elastic deformation in confined geometries that are common in lubrication problems.

As a prelude to our discussion, we consider the steady motion of a cylinder of radius R completely immersed in fluid and moving with a velocity V, with its center at height $h_0 + R$ above a rigid surface (see Fig. 1). The dynamics of the fluid of viscosity μ, and density ρ are described using the Navier-Stokes equations:

$$\rho(\partial_t \mathbf{v} + \mathbf{v} \cdot \nabla \mathbf{v}) = \mu \nabla^2 \mathbf{v} - \nabla p, \qquad (1)$$

$$\nabla \cdot \mathbf{v} = 0, \qquad (2)$$

where $\mathbf{v}$ is the 2D velocity field (u, w) and p is the pressure. Comparing the ratio between the inertial and viscous forces in the narrow gap having a contact length $l \sim \sqrt{Rh_0}$ [3], we find the gap Reynolds number $\mathrm{Re}_g = \frac{\rho V^2/l}{\mu V/h_0^2} \sim \frac{\rho V h_0^{3/2}}{\mu R^{1/2}} \ll \frac{\rho V R}{\mu} = \mathrm{Re}$, the nominal Reynolds number. The gap Reynolds number is small since $h_0 \ll R$, and

we can safely neglect the inertial terms and use the Stokes' equations (and the lubrication approximation thereof [4]) to describe the hydrodynamics. The temporal reversibility associated with the Stokes equations and the symmetry of the parabolic contact leads to the conclusion that there can be no normal force due to the horizontal motion of the cylinder. However, if there is a thin soft elastic layer on either the cylinder or the wall, the deformation of the layer breaks the contact symmetry and leads to a normal force. This then leads to an enhanced physical separation and a reduced shear so that it may be a likely cause for the low wear properties of cartilaginous joints.

Continuing our analysis in the context of a cylinder moving along a planar wall, we take the x direction to be parallel to the wall in the direction of motion of the cylinder and the z direction to be perpendicular to the wall; p is the fluid pressure; h is the distance between the solid surfaces. Guided by lubrication theory [4], we use the following scalings:

$$x = \sqrt{2h_0 R}X, \qquad z = h_0 Z, \qquad p = \frac{\sqrt{2R}\mu V}{h_0^{3/2}}P,$$
$$\qquad (3)$$
$$h = h_0 H, \qquad u = VU, \qquad w = \frac{V\sqrt{h_0}}{\sqrt{2R}}W,$$

to reduce (1) and (2) to

$$\partial_X P = \partial_{ZZ} U, \qquad \partial_Z P = 0, \qquad (4)$$

$$\partial_X U + \partial_Z W = 0. \qquad (5)$$

We consider steady motion in the reference frame of the cylinder, so that the boundary conditions are

$$U(X, 0) = -1, \qquad U(X, H) = 0,$$
$$\qquad (6)$$
$$W(X, 0) = W(X, H) = 0.$$

Integrating (4)–(6) leads to the dimensionless Reynolds equation [5]:

$$0 = \partial_X(6H + H^3\partial_X P). \qquad (7)$$

Since the gap pressure is much larger than the ambient pressure, we may approximate the boundary conditions on the pressure field as

$$P(\infty) = P(-\infty) = 0. \qquad (8)$$

Next, we consider the deformation of the elastic layer of thickness H_l that rests on a rigid support. Balance of stresses in the solid leads to

$$\nabla \cdot \boldsymbol{\sigma} = 0, \qquad (9)$$

with the stress given by

$$\boldsymbol{\sigma} = G(\nabla \mathbf{u} + \nabla \mathbf{u}^T) + \lambda \nabla \cdot \mathbf{u}\, \mathbf{I}, \qquad (10)$$

where $\mathbf{u} = (u_x, u_z)$ is the displacement field and G and λ are the Lamé constants for the solid, which is assumed to be isotropic and linearly elastic. To calculate the increase in gap thickness $H(x)$, we use the analog of the lubrication approximation in the solid layer [6]. The length scale in the z direction is H_l and the length scale in the x direction is $\sqrt{h_0 R}$. We take the thickness of the solid layer to be small compared to the thickness of the contact zone, $\sqrt{h_0 R} \gg H_l$, and consider a compressible elastic material, $G \sim \lambda$, to find the vertical force balance: $\partial_{zz} u_z = 0$. The boundary condition at the solid-fluid interface is $\boldsymbol{\sigma} \cdot \mathbf{n} = -p\mathbf{n}$, so that $(2G + \lambda)\partial_z u_z(x, 0) = -p(x)$. Using the zero displacement condition at the interface between the soft and rigid solid, $u_z(x, -H_l) = 0$ leads to the following expression for the displacement of the surface:

$$u_z(x, 0) = -\frac{H_l p(x)}{2G + \lambda}. \qquad (11)$$

The dimensionless version of the gap thickness, $h = h_0(1 + \frac{x^2}{2h_0 R} - \frac{u_z(x,0)}{h_0})$, is

$$H(X) = 1 + X^2 + \eta P(X), \qquad (12)$$

where $\eta = \Delta h/h_0 = (\sqrt{2R}H_l \mu V)/[h_0^{5/2}(2G + \lambda)]$ is the dimensionless parameter governing the size of the deflection. Inspired by the some recent experiments [7] in a similar geometry, we consider a cylinder of radius $R = 10$ cm coated with a rubber layer ($H_l = 0.1$ cm, $G = 1$ MPa) moving through water ($\mu = 1$ mPa s, $V = 1$ cm/s, $h_0 = 10^{-3}$ cm). Then $\eta = 10^{-2} \ll 1$, so that we may use the perturbation expansion $P = P_0 + \eta P_1$, where P_0 is the antisymmetric pressure distribution corresponding to an undeformed layer, and P_1 is the symmetric pressure perturbation induced by elastic deformation. Substituting (12) into (7) leads to the following equations for P_0, P_1:

$$\eta^0: \partial_X[6(1 + X^2) + (1 + X^2)^3\partial_X P_0] = 0, \qquad (13)$$
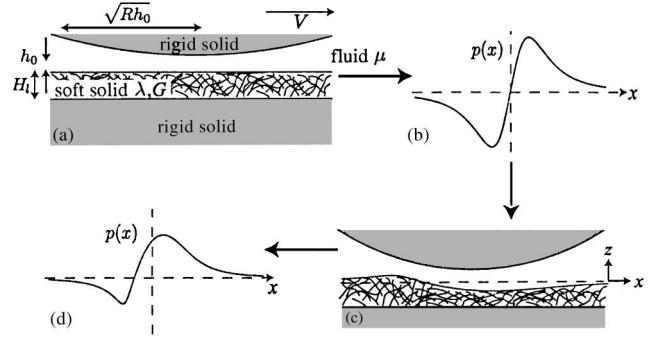
FIG. 1.   A rigid cylinder moves at a velocity V a distance h_0 above a rigid substrate coated with an elastic layer of thickness H_l. H_l, $h_0 \ll \sqrt{h_0 R} = l$. We illustrate the steps of the perturbation analysis. (b) An antisymmetric pressure distribution pushes down on the gel in front of and pulls the gel up behind the cylinder. (c) The fore-aft gap profile symmetry is broken. (d) The new pressure field produces a normal force. (a) and (b) correspond to an undeformed substrate, while (c) and (d) correspond to solutions of (7), (8), and (12) for $\eta = (\Delta h)/h_0 = 10$.

$$\eta^1: \partial_X[6P_0 + 3(1 + X^2)^2 P_0\partial_X P_0 + (1 + X^2)^3\partial_X P_1] = 0, \qquad (14)$$

subject to the boundary conditions $P_0(\infty) = P_0(-\infty) = P_1(\infty) = P_1(-\infty) = 0$. Solving (13) and (14) yields

$$P = \frac{2X}{(1 + X^2)^2} + \eta\frac{3(3 - 5X^2)}{5(1 + X^2)^5}. \qquad (15)$$

Then the normal force is

$$F = \int_{-\infty}^{\infty} P\, dX = \frac{3\pi}{8}\eta, \qquad (16)$$

In dimensional terms, $F = [(3\sqrt{2}\pi)/4]\{(\mu^2 V^2 H_l R^{3/2})/[h_0^{7/2}(2G + \lambda)]\}$, whose scaling matches the result reported in [8], but with a different prefactor. When η is not small, we solve (7), (8), and (12) numerically. Figure 2 shows that as η increases the mean gap increases and its profile becomes asymmetric, resembling the profile of a rigid slider bearing, a configuration well known to generate lift forces [4]. In addition, this increase in the gap size causes the peak pressure to decrease since $p \sim (\mu V R^{1/2})/h_0^{3/2}$. These two competing effects produce a maximum lift force when $\eta = 2.06$.

The physical basis for the previous arguments can be more easily understood using scaling and therefore allows us to generalize these results to a variety of configurations involving lubrication of soft contacts (Fig. 3; Table I). Balancing the pressure gradient in the gap with the viscous stresses yields

$$\frac{p}{l} \sim \frac{\mu V}{h^2} \rightarrow p \sim \frac{\mu V R^{1/2}}{h^{3/2}}. \qquad (17)$$

Substituting $h = h_0 + \Delta h$, with $\Delta h \ll h_0$, we find that the lubrication pressure is
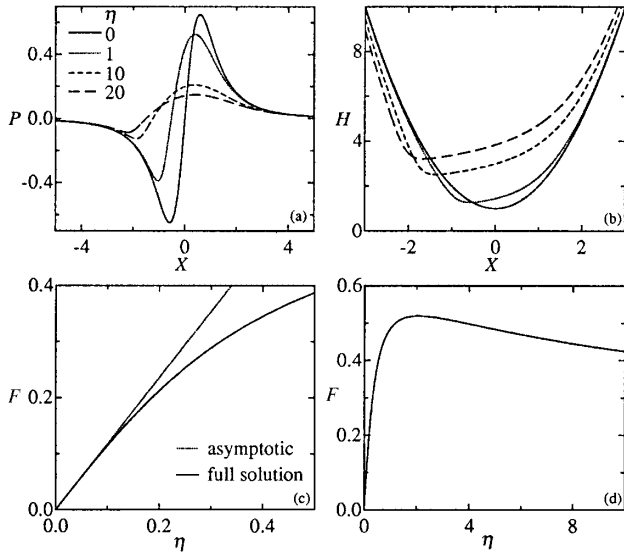
FIG. 2. (a) The dimensionless pressure distribution, P, for several values of η, a measure of the deflection of the elastic layer compared to the initial separation. (b) The dimensionless gap thickness profile, $H = 1 + X^2 + \eta P$. The gap thickness and asymmetry increase with η, while the maximum value of the pressure decreases. (c) For small η asymptotic analysis predicts a dimensionless lift force $F = [(3\pi)/8]\eta$, which matches the numerical solution. (d) F has a maximum at $\eta = 2.06$ as a result of the competition between symmetry breaking and decreasing pressure.

$$p \sim \frac{\mu V \sqrt{Rh_0}}{(h_0 + \Delta h)^2} \sim \frac{\mu V R^{1/2}}{h_0^{3/2}}\left(1 + \frac{\Delta h}{h_0}\right) = p_0 + \frac{\Delta h}{h_0} p_1.$$

$$(18)$$

Here p_0 does not contribute to the lift for the reasons outlined earlier, so that the lift on the cylinder per unit length is

$$F \sim \frac{\Delta h}{h_0} p_1 l \sim \frac{\mu V R}{h_0^2} \Delta h, \qquad (19)$$

where Δh is determined by the solution of the elasticity problem.

For a thin compressible layer, the case treated above, the normal strain is $(\Delta h)/H_l \sim p_0/G \sim (\mu V R^{1/2})/(G h_0^{3/2})$. Therefore,

$$\Delta h \sim \frac{\mu V}{G} \frac{H_l R^{1/2}}{h_0^{3/2}}, \qquad F \sim \frac{\mu^2 V^2}{G} \frac{H_l R^{3/2}}{h_0^{7/2}}. \qquad (20)$$

In sharp contrast, a thin incompressible layer will deform via shear with an effective shear strain $(\Delta u)/H_l \sim (l\Delta h)/H_l^2$ [9]. Balancing the elastic energy $\int G[(R^{1/2} h_0^{1/2} \Delta h)/H_l^2]^2 dV \sim G[(R^{1/2} h_0^{1/2} \Delta h)/H_l^2]^2 \times H_l\sqrt{Rh_0}$ with the work done by the pressure $p_0(\sqrt{h_0 R})^2 \frac{\Delta h}{R}$ yields Δh in terms of p_0. Then, (17) and (19) give

$$\Delta h \sim \frac{\mu V}{G} \frac{H_l^3}{h_0^{5/2} R^{1/2}}, \qquad F \sim \frac{\mu^2 V^2}{G} \frac{H_l^3 R^{1/2}}{h_0^{9/2}}. \qquad (21)$$

A thick layer ($H_l \gg \sqrt{h_0 R}$) may be treated as an elastic half space. The strain scales as $(\Delta h)/\sqrt{h_0 R}$ and remains appreciable in a region of size $h_0 R$. Balancing the elastic energy $\int G[(\Delta h)/\sqrt{h_0 R}]^2 dV \sim G[(\Delta h)/\sqrt{h_0 R}]^2 R h_0$ with the work done by the pressure $p_0 \Delta h \sqrt{Rh_0}$ yields Δh in terms of p_0. Then, (17) and (19) give

$$\Delta h \sim \frac{\mu V}{G} \frac{R}{h_0}, \qquad F \sim \frac{\mu^2 V^2}{G} \frac{R^2}{h_0^3}. \qquad (22)$$

Finally, we consider the case of a cylindrical shell, of radius R and thickness h_s, moving over a rigid substrate. Since the shell is thin it can be easily deformed via cylindrical bending without stretching. The bending strain is $(h_s \Delta h)/R^2$ so that the elastic energy $\int G[(h_s \Delta h)/R^2]^2 dA \sim (G h_s^3 \Delta h^2)/R^3$. Balancing this with the work done by the pressure $p_0(\sqrt{h_0 R})^2 \frac{\Delta h}{R}$ yields Δh in terms of p_0. Then, (17) and (19) give

$$\Delta h \sim \frac{\mu V}{G} \frac{R^{7/2}}{h_s^3 h_0^{1/2}}, \qquad F \sim \frac{\mu^2 V^2}{G} \frac{R^{9/2}}{h_s^3 h_0^{5/2}}. \qquad (23)$$

We note that the above scalings for cylindrical contacts can be trivially generalized to spherical contacts for the case of small deformations, but space precludes us from discussing these in detail.

We conclude with a discussion of how our results may be applied to the lubrication of cartilaginous joints [10,11], where a thin layer of a fluid-filled gel, the cartilage, coats the stiff bones and mediates the contact between them. Here, electrostatic effects prevent physical contact of the surfaces under high static normal loads, while elastohydrodynamic effects could enhance separation and thus reduce wear. Inspired by the treatment of cartilage using poroelasticity [10,12], the continuum description of a material composed of an elastic solid skeleton and an interstitial fluid [13], we treat the cartilage layer as an isotropic poroelastic material [14]. The gel can then be described by its fluid volume fraction $\alpha \sim O(1)$, drained shear modulus G and drained bulk modulus $K \sim G$, thickness H_l, permeability k, and interstitial fluid viscosity μ. Using dimensional reasoning, we can construct a poroelastic time scale,
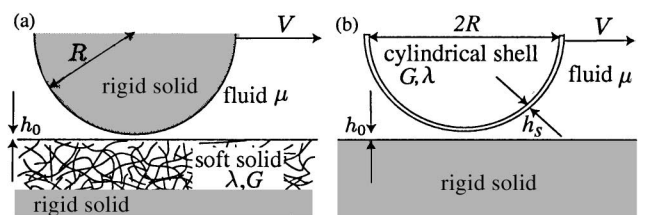

FIG. 3. Schematic diagrams of two configurations considered on the level of scaling. (a) A soft solid coats a rigid solid where $H_l \gg \sqrt{h_0 R}$, i.e., the layer thickness is larger than the length scale of the hydrodynamic interaction. (b) The cylinder is replaced by a cylindrical shell.

TABLE I. Summary of scaling results for small surface deflections.

Geometry	Material	Surface displacement	Lift force/unit length
Thin layer	Compressible elastic solid	$\dfrac{\mu V}{G}\dfrac{H_l R^{1/2}}{h_0^{3/2}}$	$\dfrac{\mu^2 V^2}{G}\dfrac{H_l R^{3/2}}{h_0^{7/2}}$
Thin layer	Incompressible elastic solid	$\dfrac{\mu V}{G}\dfrac{H_l^3}{h_0^{5/2}R^{1/2}}$	$\dfrac{\mu^2 V^2}{G}\dfrac{H_l^3 R^{1/2}}{h_0^{9/2}}$
Thin layer	Poroelastic solid	$\dfrac{\mu V}{G_{eff}}\dfrac{H_l R^{1/2}}{h_0^{3/2}}$	$\dfrac{\mu^2 V^2}{G_{eff}}\dfrac{H_l R^{3/2}}{h_0^{7/2}}$
Thick layer	Elastic solid	$\dfrac{\mu V}{G}\dfrac{R}{h_0}$	$\dfrac{\mu^2 V^2}{G}\dfrac{R^2}{h_0^3}$
Cylindrical shell	Elastic solid	$\dfrac{\mu V}{G}\dfrac{R^{7/2}}{h_s^3 h_0^{1/2}}$	$\dfrac{\mu^2 V^2}{G}\dfrac{R^{9/2}}{h_s^3 h_0^{5/2}}$

$$\tau_p \sim \frac{\mu H_l^2}{kK}, \tag{24}$$

which characterizes the time for the diffusion of stress over the layer thickness H_l due to fluid flow. Then the response of the gel is governed by the relative size of τ_p to the time scale of the motion, $\tau \sim l/V = \sqrt{h_0 R}/V$. If $\tau \gg \tau_p$, the motion is so slow that the interstitial fluid plays no role in supporting the load. If $\tau \sim \tau_p$, the fluid supports some of the load transiently, thereby stiffening the gel. Finally, if $\tau \ll \tau_p$, the response of the gel will depend on the size of the Stokes' length $l_s \sim \sqrt{\tau \mu/\rho}$. If $l_s \sim H_l$, there is no relative motion between the fluid and the solid, and the gel behaves as an incompressible elastic solid [15,16], with shear modulus G. From (20) and (21), we see that the effective modulus is

$$G_{\text{eff}} \sim p_0 H_l/\Delta h \sim \frac{l^2}{H_l^2} G \sim \frac{h_0 R}{H_l^2} G. \tag{25}$$

To find the scale of the deflection and lift force, we use the same scaling analysis as for a thin compressible elastic layer but replace G with $G_{\text{eff}}(\tau)$, so that (20) yields

$$\Delta h \sim \frac{\mu V}{G_{\text{eff}}(\tau)}\frac{H_l R^{1/2}}{h_0^{3/2}}, \qquad F \sim \frac{\mu^2 V^2}{G_{\text{eff}}(\tau)}\frac{H_l R^{3/2}}{h_0^{7/2}}, \tag{26}$$

where $G_{\text{eff}} \in \{G, [(h_0 R)/H_l^2]G\}$. Inserting characteristic values $V = 1$ cm/s, $G = 10^7$ g/s^2 cm, $H_l = 0.1$ cm, $R = 1$ cm, $h_0 = 10^{-4}$ cm, and $\frac{k}{\mu} = 10^{-13}$ cm^3 s/g shows that $\tau \ll \tau_p$, but since $l \sim H_l$ significant material stiffening is prevented. Consequently, the effective modulus is G and the scale of the deflection is

$$\eta \sim \frac{\mu V}{G}\frac{H_l R^{1/2}}{h_0^{5/2}} \sim 1, \tag{27}$$

which suggests that joints could easily operate in a parameter regime that optimizes repulsive elastohydrodynamic effects. Although our estimates are based on nonconforming contact geometries, in real joints where conforming contacts are the norm, we expect a similar if not enhanced effect.

*Current address: Division of Engineering and Applied Sciences, Harvard University, 29 Oxford Street, Cambridge, MA 02138.
Electronic address: lm@deas.harvard.edu

[1] B. J. Hamrock, *Fundamentals of Fluid Film Lubrication* (McGraw-Hill, New York, 1994).
[2] The viscosity depends on the pressure and temperature [1].
[3] All nondegenerate (nonconforming) contacts may be approximated as a parabola in the vicinity of the contact region, in which case the gap profile $h = h_0[1 + x^2/(2Rh_0)]$.
[4] G. K. Batchelor, *An Introduction to Fluid Dynamics* (Cambridge University Press, Cambridge, England, 1967).
[5] O. Reynolds, Philos. Trans. R. Soc. London **177**, 157 (1886).
[6] K. L. Johnson, *Contact Mechanics* (Cambridge University Press, Cambridge, England, 1985).
[7] A. Martin, J. Clain, A. Buguin, and F. Brochard-Wyart, Phys. Rev. E **65**, 031605 (2002).
[8] K. Sekimoto and L. Liebler, Europhys. Lett. **23**, 113 (1993).
[9] An incompressible solid must satisfy the continuity equation $\nabla \cdot \mathbf{u} = 0$, which implies that $(\Delta u/l) \sim (\Delta h/H_l)$.
[10] V. C. Mow and X. E. Guo, Annu. Rev. Biomed. Eng. **4**, 175 (2002).
[11] V. C. Mow, M. H. Holmes, and W. M. Lai, J. Biomech. **17**, 377 (1984).
[12] A. J. Grodzinsky, H. Lipshitz, and M. J. Glimcher, Nature (London) **275**, 448 (1978).
[13] M. A. Biot, J. Appl. Phys. **12**, 155 (1941).
[14] We will ignore screened electrostatic effects to leading order in the elastohydrodynamic problem.
[15] J. M. Skotheim and L. Mahadevan, Proc. R. Soc. London, Ser. A **460**, 1995 (2004).
[16] R. Burridge and J. B. Keller, J. Acoust. Soc. Am. **70**, 1140 (1981).